

Hydrogen and helium in the late phase of SNe of Type IIb

I. Maurer^{1,**}, P. A. Mazzali^{1,2,3}, S. Taubenberger¹, S. Hachinger¹

¹ *Max Planck Institut für Astrophysik, Karl-Schwarzschild-Str.1, 85741 Garching, Germany*

² *Scuola Normale Superiore, Piazza dei Cavalieri, 7, 56126 Pisa, Italy*

³ *National Institute for Astrophysics-OAPd, Vicolo dell'Osservatorio, 5, 35122 Padova, Italy*

**maurer@mpa-garching.mpg.de

30 January 2021

ABSTRACT

Supernovae of Type IIb contain large fractions of helium and traces of hydrogen, which can be observed in the early and late spectra. Estimates of the hydrogen and helium mass and distribution are mainly based on early-time spectroscopy and are uncertain since the respective lines are usually observed in absorption. Constraining the mass and distribution of H and He is important to gain insight into the progenitor systems of these SNe.

We implement a NLTE treatment of hydrogen and helium in a three-dimensional nebular code. Ionisation, recombination, (non-)thermal electron excitation and $H\alpha$ line scattering are taken into account to compute the formation of $H\alpha$, which is by far the strongest H line observed in the nebular spectra of SNe IIb. Other lines of H and He are also computed but are rarely identified in the nebular phase. Nebular models are computed for the Type IIb SNe 1993J, 2001ig, 2003bg and 2008ax as well as for SN 2007Y, which shows $H\alpha$ absorption features at early times and strong $H\alpha$ emission in its late phase, but has been classified as a SN Ib. We suggest to classify SN 2007Y as a SN IIb. Optical spectra exist for all SNe of our sample, and there is one IR nebular observation of SN 2008ax, which allows an exploration of its helium mass and distribution.

We develop a three-dimensional model for SN 2008ax. We obtain estimates for the total mass and kinetic energy in good agreement with the results from light-curve modelling found in the literature. We further derive abundances of He, C, O, Ca and ^{56}Ni . Estimates of the H mass are difficult but some constraints are derived. We demonstrate that $H\alpha$ absorption is probably responsible for the double-peaked profile of the [O I] $\lambda\lambda$ 6300, 6363 doublet in several SNe IIb and present a mechanism alternative to shock interaction for generating late-time $H\alpha$ emission of SNe IIb.

Key words:

1 INTRODUCTION

Massive stars ($> 8 M_{\odot}$) collapse when the nuclear fuel in their central regions is consumed, producing a core-collapse supernova (CC-SN) and forming a black hole or a neutron star. CC-SNe with a H-rich spectrum are classified as Type II. If the envelope was stripped to some degree prior to the explosion, the SNe are classified as Type IIb (strong He lines, and weak but clear H), Type Ib (strong He lines but no H), and Type Ic (no He or H lines) (Filippenko 1997).

Large amounts of hydrogen ($\gg 1 M_{\odot}$) cause the progenitor to become a red super-giant prior to explosion, which in turn leads to a broad peaked SN light curve (e.g. Grassberg et al. 1971). Since this is not observed in SNe of Type IIb there is an upper limit for the hydrogen mass of

less than one solar mass (Nomoto et al. 1993; Utrobin 1994; Woosley et al. 1994). It is not clear how SNe IIb manage to keep just a thin layer of hydrogen.

While massive (and therefore hot, O-Type) stars ($M > 25 M_{\odot}$) can blow off their hydrogen envelope by radiatively driven winds (e.g. Eldridge & Vink 2006), mass estimates for the progenitors of SNe IIb (e.g. Woosley et al. 1994; Mazzali et al. 2009; Silverman et al. 2009; Hamuy et al. 2009) suggest that they may not be massive enough to lose most of the H envelope via this process. Binary interaction can cause mass transfer between two interacting stars and would allow a Type IIb progenitor to lose most of its hydrogen (e.g. Woosley et al. 1994). There is observational evidence that the progenitors of SNe 1993J (Aldering et al. 1994; Maund et al. 2004; Maund & Smartt 2009), 2001ig

(Ryder et al. 2006) [also see Kotak & Vink (2006) for an alternative interpretation of the SN 2001ig data] and 2008ax (Crockett et al. 2008) may have been part of binary systems.

There is evidence of shock interaction from nebular H α (e.g. Chugai 1991; Patat et al. 1995; Houck & Fransson 1996, also see this work) as well as from radio (e.g. Fransson & Björnsson 1998; Soderberg et al. 2006; Chevalier & Soderberg 2010) and X-ray observations (e.g. Chevalier 1981; Soderberg et al. 2006; Nymark et al. 2009; Chevalier & Soderberg 2010), suggesting that at least some SNe IIB are surrounded by massive stellar winds. This wind could also be produced by the massive companion star in the binary scenario.

At early phases of SNe IIB the energy emitted by H α is probably provided by the radioactive decay chain $^{56}\text{Ni} \rightarrow ^{56}\text{Co} \rightarrow ^{56}\text{Fe}$. However, it has been shown for SN 1993J (Patat et al. 1995; Houck & Fransson 1996) that ~ 150 days after explosion this mechanism becomes ineffective suggesting that an additional source of energy is required to explain the observed H α luminosities (however this may not be true; see Section 5). A similar result had been obtained for SNe II (Chugai 1991). This is further confirmed by the detection of a flattening of the H α luminosity decay at late phases (Matheson et al. 2000). This could be inconsistent with radioactive decay, but may be explained by shock interaction.

Shock interaction can also be detected through radio and X-ray observations. As the SN ejecta propagate into the circumstellar medium, they are decelerated, creating internal energy which is dissipated by radiative processes. There are several solutions for different scenarios of shock interaction (e.g. Chevalier 1981; Suzuki & Nomoto 1995; Fransson & Björnsson 1998), but a clear interpretation of the observations is often difficult. Micro-physical processes (e.g. the formation of magnetic fields) are poorly understood, and it is not clear in detail how the energy released by the shock is transferred into radiation. The SN envelope and circumstellar density profiles are not known and have to be treated as free parameters. Several authors found evidence for inhomogeneous wind structures and deviations from wind-like density profiles of the external medium (e.g. Fransson 1994; van Dyk et al. 1994; Suzuki & Nomoto 1995). This may however be an artefact of an inaccurate treatment of shock physics (Fransson & Björnsson 1998, 2005). A very careful treatment of shock interaction seems necessary to obtain reliable results (e.g. Fransson & Björnsson 1998).

Asphericities in the inner and outer ejecta are evident in at least some CC-SNe. Three indicators are velocity differences of Fe and lighter element lines at late times (e.g. Mazzali et al. 2001), polarisation measurements (e.g. Höflich 1991) and double-peaked or asymmetric emission line profiles (e.g. Mazzali et al. 2005; Maeda et al. 2008; Modjaz et al. 2008; Taubenberger et al. 2009; Maurer et al. 2010)[also see Milisavljevic et al. (2010) for an alternative interpretation, which is however doubtful (Maurer et al. 2010)]. Indirect evidence also emerges from a comparison of the inner and outer ejecta velocities (Maurer et al. 2010). We find evidence that SN 2008ax is a non-spherical event (see Section 3).

Between 100 and 200 days after explosion most SNe enter their nebular phase. Owing to the decrease of den-

sity the SN ejecta become transparent at most wavelengths, which makes it possible to observe the innermost parts of the SN. Nebular modelling provides the opportunity to derive information about the SN ejecta mass, kinetic energy, abundances and geometry, which can hardly be obtained by other methods at least for the central regions.

Nebular observations are available for very few SNe IIB. To our knowledge there are nebular spectra of SNe 1993J, 2001ig, 2003bg, 2006T, 2008aq and 2008ax. The quality of the SN 2006T spectrum is poor. For SN 2008aq there is no light curve and therefore there are no flux-calibrated spectra. Therefore, neither SNe are included in our analysis.

Although early time H α absorption features are observed, SN 2007Y was classified as a SN Ib by Stritzinger et al. (2009), who argued there is very little hydrogen in the envelope and that the late H α emission is powered by shock interaction. On the other hand, Chevalier & Soderberg (2010) found that the H α emission of SN 2007Y must be powered by radioactive decay before 300 days after explosion. SN 2007Y is included in our analysis to investigate this contradiction and a possible re-classification.

In Section 2 we describe the implementation of hydrogen and helium in our nebular code. In Section 3 we describe a three-dimensional model of SN 2008ax, give some estimates for the total mass and kinetic energy and compare them to results available in the literature. In Section 4 we present nebular models for the SNe 1993J, 2001ig, 2003bg, 2007Y. Since nebular models for these SNe are available in the literature already and since we cannot determine their helium density we concentrate on their H α emission. In Section 5 we present a scenario alternative to shock interaction for explaining strong late-phase H α emission. In Section 6 our results are discussed.

2 H AND HE IN THE NEBULAR PHASE

In this section we describe the implementation of hydrogen and helium in our nebular code (Ruiz-Lapuente & Lucy 1992; Mazzali et al. 2001, 2007; Maurer et al. 2010). The code computes the energy deposition from the radioactive decay of ^{56}Ni and ^{56}Co in the SN ejecta, uses the energy deposited to compute ionisation and excitation, and balances this with gas cooling via line emission in a NLTE scheme. The method follows that developed by Axelrod (1980).

2.1 Hydrogen

A full NLTE treatment of hydrogen is implemented in our three-dimensional nebular code. We obtain radiative transition and ionisation rates for the hydrogen atom from analytical solutions available in the literature (e.g. Burgess 1965). Collisional rates for allowed transitions between excited levels $n > 3$ are unimportant, but are included using an approximation (van Regemorter 1962). Collisional rates between quantum levels $n = 1, 2$ and 3 are taken from Scholz et al. (1990); Callaway (1994). The 2s level is additionally connected to the ground state by two-photon decay, and the 2s and 2p levels are coupled by electron and proton collisions.

Hydrogen is ionised by non-thermal electrons (produced by Compton scattering of ^{56}Co radioactive decay γ -radiation) and by UV-radiation emitted by helium if hy-

hydrogen and helium are mixed. The electron impact ionisation rate can be obtained comparing the atomic and electronic loss-functions with the ionisation cross-sections (e.g. Axelrod 1980; Maurer & Mazzali 2010). Thermal electron collisional ionisation and recombination is not important. Excitation by non-thermal electrons is important. We compute non-thermal electron excitation rates using the approximation of Rozsnyai et al. (1980).

We compare our hydrogen and helium ionisation and non-thermal excitation rates to calculations from Hachinger et. al. (in prep.) who calculate non-thermal ionisation and excitation rates solving an energy balance equation derived from the Spencer-Fano equation (Xu & McCray 1991; Lucy 1991). Although these methods are quite different, the thermal excitation and ionisation rates at various electron and atomic densities agree to 10% – 20% for both hydrogen and helium.

For levels with principal quantum number $n > 5$ we only consider recombination (these levels are almost completely depopulated and have no influence on the nebular spectrum), while a full NLTE (de-)excitation treatment is performed for lower levels.

The $n = 2$ level of H can effectively scatter the background radiation field. This is a very important process in SNe I Ib (Houck & Fransson 1996)[Hou96] since $H\alpha$ comes into resonance with the [O I] $\lambda\lambda$ 6300, 6363 doublet, which carries an important fraction of the nebular flux. The optical depth of transitions between levels $n \geq 3$ is too low to cause observable line scattering at late epochs.

Clumping of hydrogen is usually neglected in SNe I Ib (Patat et al. 1995; Houck & Fransson 1996; Mazzali et al. 2009), but it can increase the optical depth of $H\alpha$ considerably. Under certain conditions, as we show in Section 5, it can also increase the $H\alpha$ emission significantly.

2.2 Helium

Accurate atomic data for He are available in the literature (e.g. see TIPTOPbase ¹, NIST ²). For technical reasons it was more convenient for us to calculate the He radiative transition and ionisation rates using a quantum defect method (Bates & Damgaard 1949; Seaton 1958; Burgess & Seaton 1960)[also see Maurer & Mazzali (2010) for an application to oxygen], which is very accurate for helium. The disagreement between the calculations and NIST recommended data is a few percent in the worst case, having no observable influence on the line calculations.

Thermal electron excitation rates for all quantum levels $n < 4$ are taken from Berrington & Kingston (1987). The $2s(^1S)$ level is connected to the ground state by two-photon emission (2PE) (e.g. Drake et al. 1969), which turns out to be important in the nebular phase of SNe of Type I Ib (in the early phase radiative excitation of the $2p$ levels allows effective de-excitation via the $2p \rightarrow 1s$ transition, which can be more important than 2PE then).

Helium is mainly ionised by non-thermal electrons (see hydrogen). The recombination rates into all levels $n \leq 4$ are calculated by simulating recombination into and cascading

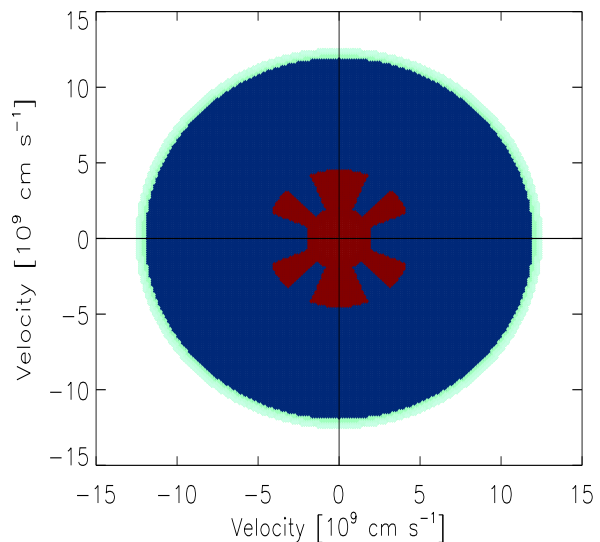


Figure 1. Illustration of the three-dimensional model of SN 2008ax, described in the text. Regions drawn in red colour are rich in heavy elements and contain no helium. Regions indicated in blue are helium-rich. The outermost region, indicated in green, is hydrogen-dominated. The x-axis is associated with the equator. In the centre (below 4500 km s^{-1}), heavy elements (red) are concentrated towards the pole, while ejecta containing helium (blue) are concentrated in the equatorial regions.

from excited levels $n \leq 30$. Levels with $n \leq 4$ are treated in full NLTE. Non-thermal electron excitation is important and is included using the approximation of Rozsnyai et al. (1980).

Helium can be observed in emission during the nebular phase of SNe I Ib since its mass is large and since it is distributed down to a few thousand km s^{-1} . Owing to the large excitation potential of He ($\sim 20 \text{ eV}$), an important fraction of the deposited energy can be radiated away by other elements which may be present in small fractions. This means that the electron temperature decreases and the He lines become weaker while the other elements emit more strongly. Since all optical He lines are blended with lines only the IR He I 10830 \AA and 20587 \AA lines can be identified clearly (at least in SN 2008ax), which allows an estimate of the He mass and distribution. Since both lines are optically thick around 100 days after explosion, they can be influenced by line scattering.

3 SN 2008AX

Nebular spectra of SN 2008ax are available at 131, 149, 266, 280 and 359 days after explosion. The spectrum at 131 days covers the range between 9000 and 25000 \AA . The other spectra cover a range between 5000 and 10000 \AA . For the modelling we use a distance modulus of $\mu = 29.92 \pm 0.29 \text{ mag}$ and an extinction of $E(B - V) = 0.4 \pm 0.1 \text{ mag}$ (see Taubenberger et al. 2010)[Tau10]. Also see Pastorello et al. (2008); Chornock et al. (2010) for observations and discussion of SN 2008ax.

¹ <http://cdsweb.u-strasbg.fr/topbase/>

² <http://www.nist.gov/index.html>

Table 1. SN 2008ax. (A) Best fit three-dimensional model (B) All ^{56}Ni confined below 2800 km s^{-1} ; inconsistent with nebular Fe-group line observations. Hydrogen is not included in the total mass and kinetic energy estimate in both models but should be of the order of $0.1 M_{\odot}$ and 10^{50} ergs.

| | He M_{\odot} | C M_{\odot} | O M_{\odot} | Ca M_{\odot} | Ni M_{\odot} | M_{Tot} M_{\odot} | E_{K} 10^{51} ergs |
|---|-------------------|------------------|------------------|-------------------|-------------------|---------------------------------|----------------------------------|
| A | 2.0 | 0.09 | 0.51 | 0.005 | 0.10 | 2.7 | ≥ 0.9 |
| B | 2.7 | 0.07 | 0.40 | 0.002 | 0.07 | 3.3 | ≥ 1.2 |

Table 2. Properties of SN 2008ax obtained by different methods: (A) Multi-dimensional nebular modelling (B) one-zone light-curve calculation (C) semi-analytical light-curve modelling (D) numerical light-curve modelling using the radiation transport code STELLA on a SN IIB explosion model (E) light-curve comparison of SN 2008ax and SN 1993J.

*Please note that (C), (D) and (E) are computed for $E(B - V) = 0.3$ mag instead of 0.4 mag. In rough approximation a comparison can be made by multiplying all quantities of (C), (D) and (E) by a factor of 1.15. These values are given in brackets.

| | μ mag | $E(B - V)$ mag | $M_{^{56}\text{Ni}}$ M_{\odot} | $M_{\text{Tot,ej}}$ M_{\odot} | E_{K} 10^{51} ergs | Reference |
|---|------------------|-------------------|-------------------------------------|------------------------------------|----------------------------------|--------------------------|
| A | 29.92 ± 0.29 | 0.4 ± 0.1 | $0.10^{+0.05}_{-0.03}$ | $2.8^{+1.2}_{-0.9}$ | $1.0^{+1.1}_{-0.3}$ | This work |
| B | 29.92 ± 0.29 | 0.4 ± 0.1 | 0.07–0.15 | 4.6 ± 2.5 | 1.0–10 | [Tau10] |
| C | 29.92 | 0.3 | $\sim 0.06^*$ [0.07] | $\sim 2.9^*$ [3.3] | $\sim 0.5^*$ [0.6] | Roming et al. (2009) |
| D | 29.92 | 0.3 | $\sim 0.11^*$ [0.13] | $\sim 2.3^*$ [2.7] | $\sim 1.5^*$ [1.7] | Tsvetkov et al. (2009) |
| E | 29.92 ± 0.29 | 0.3 | $0.07^* - 0.11^*$ [0.08 - 0.13] | $3^* - 6^*$ [3 - 7] | $\sim 1.0^*$ [1.2] | Pastorello et al. (2008) |

There is observational evidence for asymmetry in SN 2008ax. The double-peaked profiles of the He I IR 10830 and 20587 Å lines can be interpreted as a torus-shaped distribution of helium [Tau10;Chornock et al. (2010)]. In addition, the blue wing of these lines is stronger, which can be interpreted as an asymmetry along the line of sight, but may also be a scattering effect. We place the observer in the equatorial plane, which is necessary to produce the double-peaked He profiles in this model.

The choice of this geometry (see Figure 1 for illustration) is motivated by the observations but is probably not unique. Different geometries may reproduce acceptable fits to the observations as well.

In contrast to the He IR lines (see Figure 2), most other lines are single peaked (see Figure 3). This is expected, since heavy elements are concentrated in the core. An exception is the [O I] $\lambda\lambda$ 6300, 6363 doublet. While we agree that the profile of these lines may be shaped by geometry [Tau10] in other types of CC-SNe (e.g. Mazzali et al. 2005; Maeda et al. 2008; Modjaz et al. 2008; Taubenberger et al. 2009; Maurer et al. 2010), we think that in SNe IIB $H\alpha$ line scattering is responsible for the splitting of the [O I] $\lambda\lambda$ 6300, 6363 doublet (also see Section 4 for other SNe IIB).

The velocity of the $H\alpha$ absorption minimum saturates at $\sim 12500 \text{ km s}^{-1}$ about 40 days after explosion. This is usually interpreted as the lower boundary of hydrogen. Since hydrogen in lower layers may be strongly ionised (see Appendix A), this estimate is somewhat uncertain. It may rather be the lower boundary of H I but not of H II.

We can reproduce the double-peaked profile of the [O I] $\lambda\lambda$ 6300, 6363 doublet very well placing less than $0.1 M_{\odot}$ of hydrogen between 12000 and 12500 km s^{-1} (see Figure 3). An exact estimate of the H mass is not possible since shock interaction or clumping may be important in this region.

This can explain why other lines, like [O I] 5577 Å are single-peaked. This is discussed in more detail in Section 6.

Our model consists of 128 angular and 8 radial cells (spherical geometry; 1024 cells in total). The radial cells have outer boundaries at 2000, 2800, 4500, 6000, 6600, 9500, 12000 and 12500 km s^{-1} . This choice relates to the physical properties of our model for SN 2008ax.

Below 2000 km s^{-1} the ejecta are spherically symmetric. This innermost part of the SN is dominated by ^{56}Ni , oxygen and calcium. The total mass and mass fractions in this zone are quite uncertain, but their contribution to the global properties of the SN is small. No He is present ($< 10^{-4} M_{\odot}$).

The region between 2000 and 2800 km s^{-1} is similar to the innermost part, but some cells, preferentially in the equatorial plane, contain small fractions of He ($\sim 10^{-3} M_{\odot}$). The bulk of the oxygen, calcium and carbon of SN 2008ax is located in this region. In contrast to calcium, carbon is probably not present below 2000 km s^{-1} . The confinement of C to a thin low velocity layer is in agreement with theoretical predictions (e.g. Nomoto et al. 1993).

The region between 2800 and 4500 km s^{-1} is dominated by oxygen and ^{56}Ni in some cells and by He in others. This separation improves the reproduction of the observations. On the one hand He emission can be observed down to 2000 km s^{-1} and the He IR line ratio suggests that there is no strong mixing with heavy elements (which decreases the electron temperature and influences the strength and ratio of the He I 10830 and 20587 Å lines). On the other hand, the iron lines observed are much broader than 2800 km s^{-1} . Placing all the ^{56}Ni mass necessary to reproduce the observed flux below 2800 km s^{-1} causes too narrow and too strong Fe emission lines. A good compromise is found by allowing a separation of the ^{56}Ni and He-rich ejecta. Large-scale structures of burned and unburned material are not

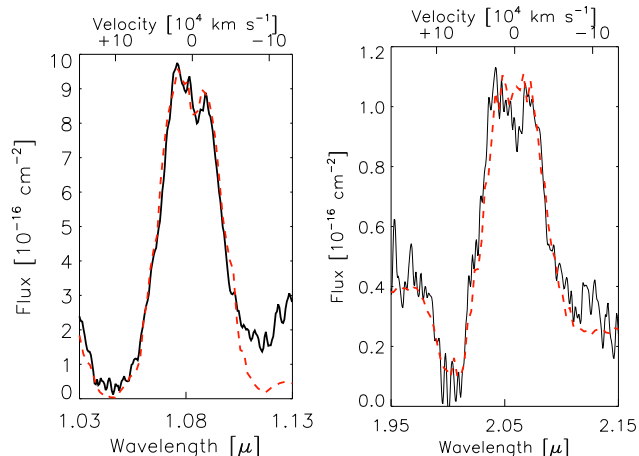


Figure 2. IR spectrum of SN 2008ax at 131 days after explosion. The He I 10830 Å line is shown on the left and the He I 20587 Å line is shown on the right. The observations are shown in black while the synthetic flux is shown by the dashed red line. The synthetic flux is obtained using the three-dimensional model described in the text. Since almost no background flux is produced by our nebular code near 20000 Å we added some constant flux at the level of the observations between 19000 and 22000 Å to allow He I 20587 Å line scattering. In contrast to the optical He lines, the 10830 Å and 20587 Å lines can be identified clearly, which allows a determination of the He density field. Two kinds of asymmetry can be observed. First, the double-peaked nature suggests a torus-shaped distribution of He. Second, the blue side of the profiles of both lines is stronger, which suggests an asymmetry along the line of sight.

unexpected depending on the explosion scenario. The He rich cells contain some fraction of carbon, oxygen, sodium and calcium (in total $\sim 30\%$). These elements are strongly excited by the energy absorbed by the He layer.

The material above 4500 km s^{-1} is dominated by helium, which constitutes most of the mass of SN 2008ax. The He rich layer reaches out to at least $\sim 9500 \text{ km s}^{-1}$. The composition and density of the zone between 9500 and 12000 km s^{-1} is not clear. The absorption profile of the He I IR lines suggests that there is no He I 20587 Å line scattering above $\sim 10000 \text{ km s}^{-1}$ (see Figure 2). An upper limit to the He mass in this region is $\sim 0.05 M_{\odot}$. The observation of the [O I] $\lambda\lambda$ 6300, 6363 doublet shows that there is no strong H α line scattering below 12000 km s^{-1} (see Figure 3). A possible solution may be that there is some He (of the order of $0.1 M_{\odot}$) in this region, but mixed with small fractions of neutral elements, like H I. In this case continuum destruction of He I 584 Å photons could reduce the optical depth of the He I 20587 Å line significantly (Chugai 1987; Li & McCray 1995). This effect strongly depends on the composition of the He layer. However, since the mass in this region is expected to be low, the effect on our total mass estimate would presumably be less than 10%. The estimate of the kinetic energy could be influenced more strongly.

The 266, 280 and 359 day H α observations cannot be reproduced using any reasonable amount of hydrogen (of the order of $0.1 M_{\odot}$). It seems likely that some additional mechanism of H α emission becomes important between 150 and 200 days after explosion, as in SN 1993J [Hou96]. In

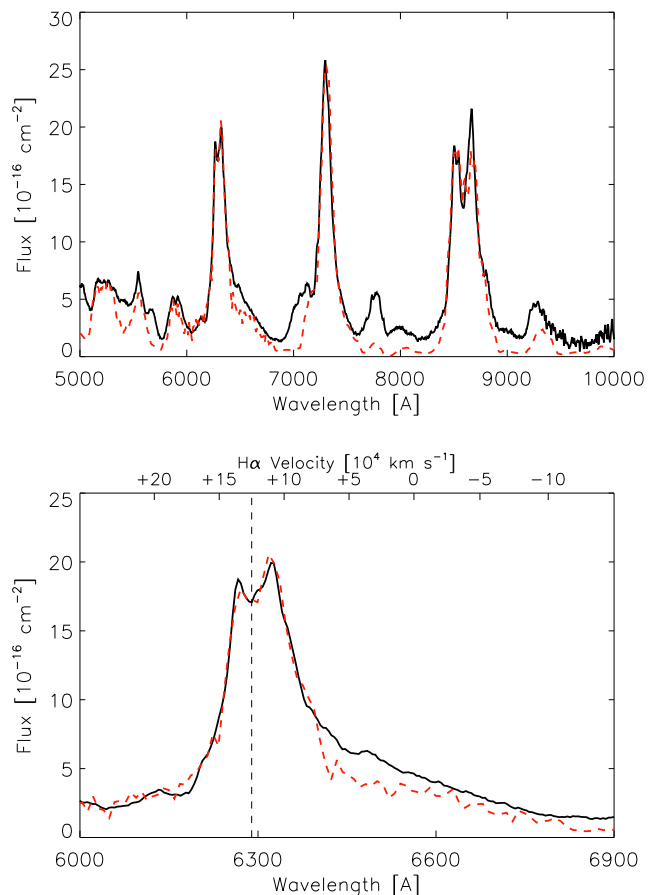


Figure 3. Optical spectrum of SN 2008ax at 149 days after explosion. Observations are shown in black while the synthetic flux is shown by the dashed red line. The synthetic flux is obtained using the three-dimensional model described in the text. Although the He I IR lines are shaped by the torus-like He distribution, all other lines are single peaked, since the heavy elements are concentrated in the core. The (double) peak of the [O I] $\lambda\lambda$ 6300, 6363 doublet profile is caused by H α absorption between ~ 12000 and 12500 km s^{-1} . The H α absorption minimum is indicated by the vertical dashed line. There seems to be continuum flux, especially between 7000 and 10000 Å , which is not reproduced. This is because of the epoch (149 days), which is too early for a strictly nebular treatment.

Section 5 we propose a mechanism, based on mixing and clumping of hydrogen and helium. Shock interaction is also a possibility and is discussed in Section 6.

The O I 7774 Å line is reproduced well at 266 days and later but is too weak at 149 days after explosion, which is expected (Maurer & Mazzali 2010) since there is no clumping of the ejecta in our model.

The He I 10830 Å line may contain some contribution from Si and S lines. However, in SN 2008ax this contribution is weak. It seems likely that He I 20583 Å and possibly He I 10830 Å are influenced by line scattering. Both lines have optical depths larger than one around 130 days after explosion. However, it is not clear if there is enough flux that can be scattered. Our nebular code produces almost no emission on the blue side of both lines. However, at least for He I 20587 Å this is in conflict with the observations, which

show some background flux around 20000 Å. Since the spectrum at 131 days is probably not completely nebular, it is not surprising that certain features of the spectrum are not reproduced well (also see the background flux in the optical spectrum at 149 days).

To handle this problem we introduce some artificial background flux between 19000 and 22000 Å at the flux level of the observations. This allows the He I 20587 Å line to increase by line scattering. However, since this background is completely artificial, one can not expect that the modelling is accurate.

The masses estimated for He, C, O, Ca and ^{56}Ni are shown in Table 1. The uncertainties on these estimates should be of the order of (several) 10%. Other elements carry larger uncertainties. We also compute the total mass and kinetic energy, excluding hydrogen. Our best-fit three-dimensional model is listed Table 1, row (A). Since some SN I Ib models predict a confinement of ^{56}Ni to quite low velocities (Nomoto et al. 1993), we additionally show an estimate obtained by placing all ^{56}Ni below 2800 km s $^{-1}$ (B), which is, however, in conflict with the Fe-group emission line observations.

A comparison of the total mass of models (A) and (B) shows that the uncertainties owing to the distribution of ^{56}Ni is about half a solar mass. However, since model (B) stands in clear contradiction to the nebular Fe-group emission line observations model (A) has to be preferred. There are also uncertainties from He I background scattering, clumping and from the atomic data. Additionally, we may underestimate the mass in the outer regions.

Owing to all the uncertainties described above, we estimate a total mass between 2.2 and 3.2 M_{\odot} and a ^{56}Ni mass between 0.10 and 0.12 M_{\odot} . A lower limit on the kinetic energy is $0.9 \cdot 10^{51}$ ergs (for a total mass of 2.7 M_{\odot}). Since small amounts of high velocity H and He could increase the total kinetic energy considerably we estimate a total kinetic energy between 0.7 and $1.7 \cdot 10^{51}$ ergs (for a total mass between 2.2 and 3.2 M_{\odot}).

In addition there is some uncertainty ($\sim 40\%$) owing to extinction (we used $E(B - V) = 0.4 \pm 0.1$ mag) and distance (9.6 ± 0.3 Mpc). Since these uncertainties would influence the total mass and the ^{56}Ni mass estimate simultaneously we assume that the uncertainty owing to distance and extinction is $\sim 20\%$ on each of these quantities. Thus we estimate (including 0.1 M_{\odot} of hydrogen with a kinetic energy of 10^{50} ergs) a total mass of $2.8_{-0.9}^{+1.2}$ M_{\odot} , a total ^{56}Ni mass of $0.10_{-0.03}^{+0.05}$ and a total kinetic energy $1.0_{-0.3}^{+1.1} \cdot 10^{51}$ ergs.

In Table 2 we compare our estimates to results from other groups. [Tau10] obtain estimates from one-zone-modelling of the light curve. They estimate a total mass of ~ 4.6 M_{\odot} , a kinetic energy of $6 \cdot 10^{51}$ ergs and a ^{56}Ni mass of 0.1 M_{\odot} . The estimates of the total mass and kinetic energy are larger than found in this work. The uncertainties estimated by [Tau10] are large and the results agree within these uncertainties. Roming et al. (2009) model the light-curve of SN 2008ax using a combination of an analytical light-curve model and a Monte-Carlo routine. Our results are roughly consistent, however the kinetic energy estimated by Roming et al. (2009) seems to be too low in general. This has also been found by [Tau10].

A comparison to Tsvetkov et al. (2009) shows that our

results agree rather well. Since the extinction was estimated to be lower in the work of Tsvetkov et al. (2009) we multiply their results by a factor of 1.15 for comparison. This gives 0.127 M_{\odot} of ^{56}Ni , a total mass of 2.7 M_{\odot} and a kinetic energy of $1.7 \cdot 10^{51}$ ergs. We may underestimate the kinetic energy but our results agree within the errors.

Our estimates for the ^{56}Ni and total mass, as well as for the kinetic energy are also consistent with the results of Pastorello et al. (2008).

4 OTHER SNE OF TYPE IIB

Nebular models for SNe 1993J [Hou96], 2001ig (Silverman et al. 2009), 2003bg (Mazzali et al. 2009) and 2007Y (Stritzinger et al. 2009) exist but a treatment of helium was not possible, since there are no IR nebular spectra ([Hou96] included He in their analysis but had no IR observations for comparison). An exact treatment of hydrogen is also difficult since it is observed as H α , which may be influenced by scattering, clumping and shock interaction.

Therefore, we restrict our analysis to the question: can H α be powered by radioactive energy deposition, as described by [Hou96]? The answer to this question is less model dependent than estimating element masses or distributions. At late epochs (> 200 days) the SN ejecta are illuminated homogeneously by γ -radiation (since the γ -optical depth is low) and asymmetries in the ^{56}Ni or hydrogen distribution are not very important. In addition we can obtain some constraints on the H and He distribution from early and late-time line-width observations. The maximum H mass is restricted by light curve observations and should be less than one solar mass (Nomoto et al. 1993; Utrobin 1994; Woosley et al. 1994).

Early time observations show that all SNe of our sample have absorption minima of H α between 13000 and 20000 km s $^{-1}$ during the first days after explosion. The velocity of these absorption minima decreases rapidly in the following tens of days and bottoms out at $\sim 10000 - 13000$ km s $^{-1}$ in all SNe around 30 – 40 days after explosion. This saturation behaviour is usually interpreted as the lower boundary of the hydrogen layer. However, there may be some hydrogen at lower velocities if it is ionised completely in the early phase of the SN (see Appendix A). We show that there is an intriguing link between the velocity of the early time H α absorption minimum and the profile of the [O I] $\lambda\lambda$ 6300, 6363 doublet for all SNe of our sample (see Table 3).

Whether a double-peaked [O I] $\lambda\lambda$ 6300, 6363 doublet is formed or not, depends on the velocity of the optically thick H α . The optimum H α velocity to produce a double-peaked O [I] profile is ~ 12000 km s $^{-1}$ since then the absorption minimum of H α for 6300 Å lies right at the centre of the [O I] λ 6300 line profile, which corresponds to the centre of the SN (bulk of oxygen).

4.1 SN 1993J

Nebular spectra of SN 1993J have been modelled before, investigating the formation of the H α line in detail [Hou96]. We repeat this analysis to test whether our results are in agreement with previous findings. We have spectra at 118,

Table 3. The velocity of the absorption minimum of $H\alpha$ at ~ 40 days after the explosion ($v_{\text{phot},H\alpha}$) taken from the literature and the velocity of the $H\alpha$ derived from the [O I] $\lambda\lambda$ 6300, 6363 doublet profile in this work ($v_{\text{neb},H\alpha}$). A physical connection between both velocities seems likely, confirming that the profile of the [O I] $\lambda\lambda$ 6300, 6363 doublet is strongly influenced by $H\alpha$ absorption.

| SN | $v_{\text{phot},H\alpha}$ km s $^{-1}$ | $v_{\text{neb},H\alpha}$ km s $^{-1}$ | M_{H} M_{\odot} | Reference |
|--------|---|--|-------------------------------|-----------------------|
| 1993J | ~ 10000 | ≤ 11000 | ~ 0.2 | Woosley et al. (1994) |
| 2001ig | ~ 13500 | ~ 13200 | – | Maund et al. (2007) |
| 2003bg | ~ 13000 | ~ 12800 | ≥ 0.05 | Mazzali et al. (2009) |
| 2007Y | ~ 10000 | ≤ 11000 | – | [Tau10] |
| 2008ax | ~ 12500 | ~ 12200 | – | [Tau10] |

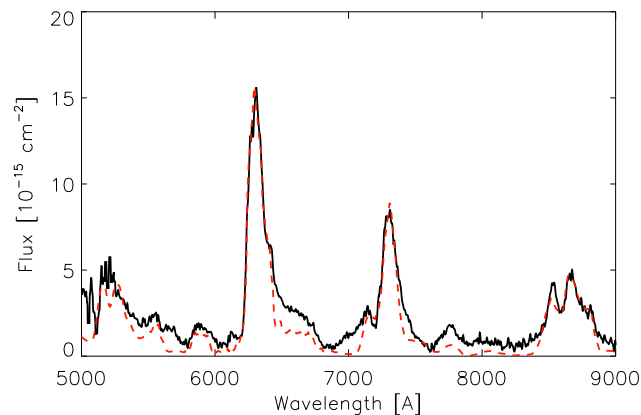


Figure 4. Optical spectrum of SN 1993J at 206 days after explosion (black line). The synthetic flux (red dashed line) is produced using $0.2 M_{\odot}$ of hydrogen distributed between 7000 and 10000 km s $^{-1}$. $H\alpha$ is not reproduced with sufficient strength. The [O I] $\lambda\lambda$ 6300, 6363 doublet is single peaked, since hydrogen is located below 11000 km s $^{-1}$.

172, 206, 237, 256, 300 and 363 days after explosion. While the 118 day spectrum is not strictly nebular, all the later ones are. The spectra cover a range between 4000 and 10000 Å but no IR observations are available. For the modelling we use a distance modulus of $\mu = 27.72$ mag and an extinction of $E(B - V) = 0.18$ mag [Hou96].

[Hou96; see their Figure 1] have shown that a model consisting of a heavy element core ($0 - 3400$ km s $^{-1}$), a He layer ($3400 - 7800$ km s $^{-1}$) and a hydrogen dominated layer (> 7800 km s $^{-1}$) containing $\sim 25\%$ of He can produce synthetic spectra consistent with the nebular observations of SN 1993J (except $H\alpha$ at late epochs).

Using a model similar to the one presented by [Hou96] we can reproduce the evolution of the heavy element lines of SN 1993J at all epochs between 118 and 363 days (e.g. see Figure 4). The hydrogen mass of SN 1993J was estimated to be $0.2 M_{\odot}$ (Woosley et al. 1994; Houck & Fransson 1996). Using this hydrogen mass we come to the same conclusions as [Hou96]. The synthetic $H\alpha$ flux and the observations become inconsistent between 150 and 200 days after explosion. This is usually interpreted as the time of the transition to

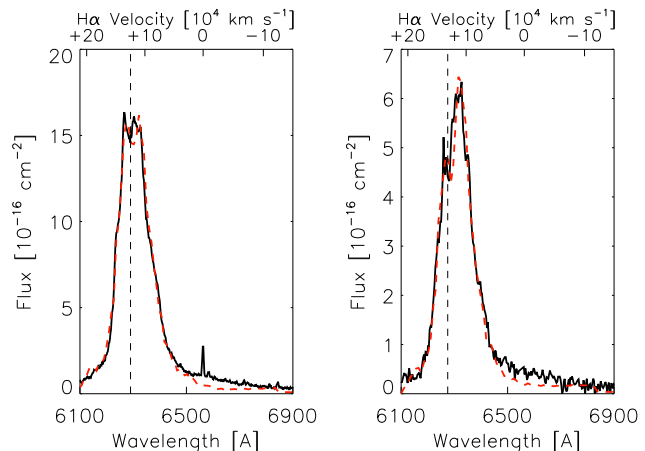


Figure 5. Left: Optical spectrum of SN 2001ig at 340 days after explosion. Right: Optical spectrum of SN 2003bg at 301 days after explosion. The band shown (6100 to 6900 Å) is dominated by the [O I] $\lambda\lambda$ 6300, 6363 doublet. The observations are shown by the black lines. The red dashed lines show the synthetic flux obtained using $\sim 0.3 M_{\odot}$ of hydrogen and a **one-dimensional** model. Hydrogen causes some weak line scattering of the oxygen-dominated flux around 6300 Å, creating the double peaked profile of the oxygen doublet, but does not provide enough $H\alpha$ flux to explain the observations around 6560 Å. The double peaked oxygen profile is not caused by geometry, but by $H\alpha$ absorption around 13200 km s $^{-1}$ (SN 2001ig) and 12800 km s $^{-1}$ (SN 2003bg). The $H\alpha$ absorption minima are indicated by the vertical dashed lines.

a shock interaction dominated phase (e.g. Patat et al. 1995; Houck & Fransson 1996).

The [O I] $\lambda\lambda$ 6300, 6363 line in SN 1993J is not double-peaked. As we have shown for SN 2008ax, the double-peaked oxygen profile is possibly the result of $H\alpha$ absorption. Since the optically thick $H\alpha$ of SN 1993J has a velocity < 11000 km s $^{-1}$ (see Table 3), the oxygen line is not split by the $H\alpha$ absorption minimum. This is discussed in more detail in Section 6.

4.2 SNe 2001ig & 2003bg

For SN 2003bg there is a H mass estimate of $\sim 0.05 M_{\odot}$ obtained from early-time absorption modelling (Mazzali et al. 2009), while there is no estimate of the H mass of SN 2001ig.

We have nebular spectra of SN 2001ig at 256, 309 and 340 days after explosion. The spectra cover a range between 4000 and 10000 Å. For the modelling we use a distance modulus of $\mu = 30.5$ mag and an extinction of $E(B - V) = 0.011$ mag (Silverman et al. 2009).

For SN 2003bg we have nebular spectra at 264 and 301 days after explosion. The spectra cover a range between 4000 and 10000 Å. For the modelling we use a distance modulus of $\mu = 31.68$ mag and an extinction of $E(B - V) = 0.02$ mag (Mazzali et al. 2009).

Although the nebular $H\alpha$ flux is weak in both SNe, we find that it cannot be reproduced using reasonable amounts of hydrogen. In contrast to the $H\alpha$ emission, the absorption can be reproduced well. The [O I] $\lambda\lambda$ 6300, 6363 doublet is often used to investigate asymmetries of CC-SNe cores. However, in the case of SNe IIB there is strong evidence

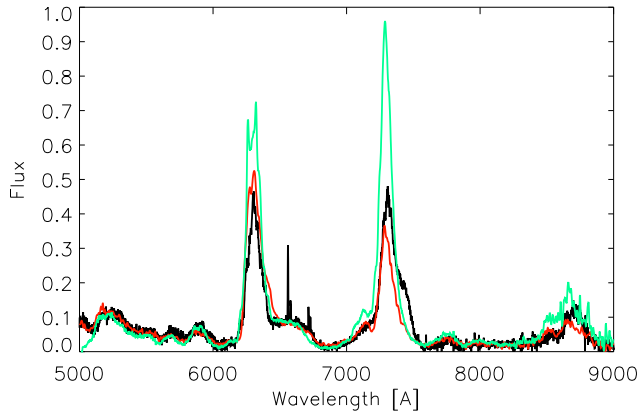


Figure 6. Optical spectra of SNe 1993J (256 days; red line), 2007Y (248 days; black line) and 2008ax (266 days; green line). The spectra are scaled by arbitrary constants. Apart from the [O I] $\lambda\lambda$ 6300, 6363 doublet and the [Ca II] emission the spectra agree extremely well. The ratio of $H\alpha$ to oxygen emission is strongest in SN 2007Y, which is surprising since this SN was classified as SN Ib, while SNe 1993J and 2008ax were classified as Type IIb. SN 2007Y has the strongest nebular ratio of $H\alpha$ to oxygen (and total) flux ever detected in a stripped CC-SN. The [O I] $\lambda\lambda$ 6300, 6363 doublet is single-peaked, which is expected if the bulk of hydrogen is located below 11000 km s^{-1} .

that the profile of the oxygen line is not shaped by geometry alone but also by absorption (see Section 3). To reproduce the oxygen profiles of SN 2001ig and 2003bg we have to place $\sim 0.3 M_{\odot}$ of hydrogen between 13000 and 13500 km s^{-1} (SN 2001ig) and 12600 and 13000 km s^{-1} (SN 2003bg) which is roughly consistent with the early-time absorption minimum of $H\alpha$ (see Table 3) of these SNe.

Although we can reproduce the absorption features well, it seems unlikely that $0.3 M_{\odot}$ of hydrogen are necessary to reproduce the observations if there is some additional mechanism of $H\alpha$ excitation (e.g. shock interaction). This may be expected, since $H\alpha$ emission is underestimated in our models.

4.3 SNe 2007Y

Although $H\alpha$ absorption was detected in its early spectra, SN 2007Y was classified as a SN Ib (Stritzinger et al. 2009). While these $H\alpha$ features would be sufficient to classify SN 2007Y as a Type IIb, there is more evidence for the presence of hydrogen since there is strong $H\alpha$ emission in the nebular phase. Stritzinger et al. (2009) argue that the emission is caused by shock interaction, but Chevalier & Soderberg (2010) claim that the circumstellar density of SN 2007Y is too weak to produce the $H\alpha$ luminosities observed before 300 days after explosion.

The nebular spectra cover a range between 4000 and 10000 \AA . For the modelling we use a distance modulus of $\mu = 31.43 \text{ mag}$ and an extinction of $E(B - V) = 0.112 \text{ mag}$ (Stritzinger et al. 2009). There is no IR nebular spectrum.

The $H\alpha$ flux can be reproduced neither at 248 nor at 288 days using reasonable amounts of hydrogen. We therefore conclude that the $H\alpha$ flux of SN 2007Y cannot result from

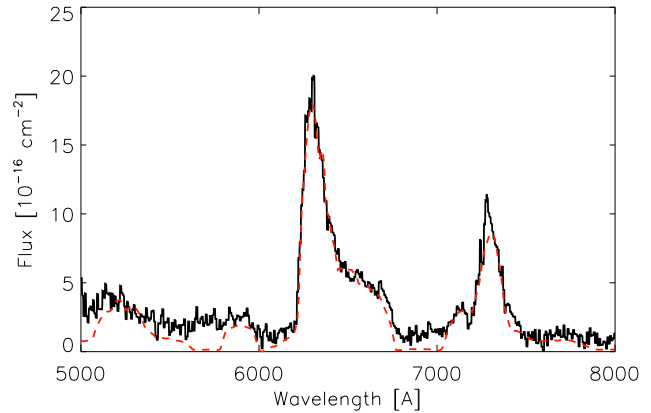


Figure 7. Optical spectrum of SN 1993J at 363 days after explosion (black line). The synthetic flux (red dashed line) was produced by a one-dimensional model containing $2 M_{\odot}$ of He and $0.2 M_{\odot}$ of hydrogen. H and He are mixed and distributed out to $\sim 10000 \text{ km s}^{-1}$. A clumping factor of the He layer of $\zeta = 200$ was used. As expected the [O I] $\lambda\lambda$ 6300, 6363 doublet is single peaked.

radioactive energy deposition as described by [Hou96] even if it was a SN IIb and that some other mechanism is needed. To avoid a double-peaked profile of the [O I] $\lambda\lambda$ 6300, 6363 doublet, the hydrogen must be concentrated below 11000 km s^{-1} . This is in perfect agreement with observations of the early-time $H\alpha$ absorption minimum (see Table 3).

SN 2007Y has the highest $H\alpha$ to [O I] $\lambda\lambda$ 6300, 6363 doublet flux ratio (and also total flux) of all five SNe (see Figure 6). Unless a serious amount of hydrogen has been accreted from a thick circumstellar wind, SN 2007Y must have had a significant fraction of H in its outer layers at the time of explosion. In addition, $H\alpha$ is observed at $\sim 15000 \text{ km s}^{-1}$ during the first days after explosion.

Therefore, SN 2007Y is most likely a SN of Type IIb similar to SN 1993J and SN 2008ax. Then it is important to understand why the early time $H\alpha$ absorption was weak (Stritzinger et al. 2009). A simple explanation may be that the hydrogen of SN 2007Y is more mixed with helium than the hydrogen of SN 1993J and 2008ax. In this case hydrogen could be ionised more strongly at early times, which means that there is hydrogen but no H I. Thorough mixing of hydrogen and helium could also explain the strong, low-velocity $H\alpha$ emission observed at late epochs (see Section 5). This is discussed in more detail in Section 6.

5 AN ALTERNATIVE TO SHOCK INTERACTION

To our knowledge there are only three stripped CC-SNe (SNe 1993J, 2007Y, 2008ax) which show strong, box-shaped $H\alpha$ emission in their nebular phase. It is commonly assumed (e.g. Filippenko et al. 1994; Patat et al. 1995; Houck & Fransson 1996) that the box-shaped $H\alpha$ emission of SN 1993J is caused by shock interaction.

[Hou96] have shown that radioactive energy deposition is too weak to produce strong $H\alpha$ emission at late epochs.

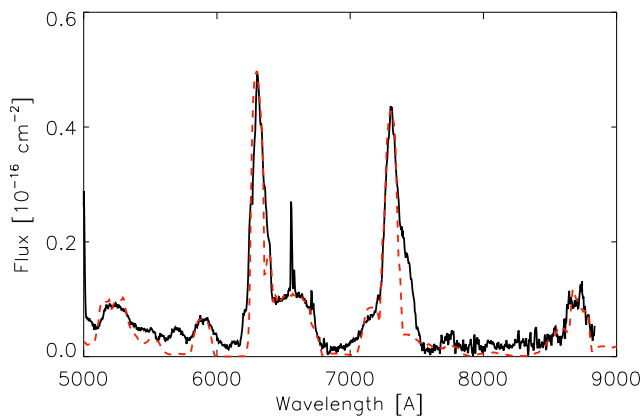


Figure 8. Optical spectrum of SN 2007Y at 288 days after explosion (black line). The synthetic flux (red dashed line) was produced by a one-dimensional model containing $1.5 M_{\odot}$ of He and $0.1 M_{\odot}$ of hydrogen. H and He are mixed and distributed out to $\sim 10500 \text{ km s}^{-1}$. A clumping factor of the He layer of $\zeta = 100$ was used. As expected the [O I] $\lambda\lambda$ 6300, 6363 doublet is single peaked.

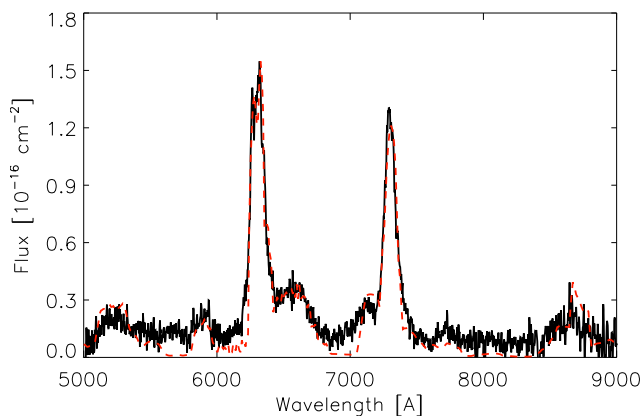


Figure 9. Optical spectrum of SN 2008ax at 359 days after explosion (black line). The synthetic flux (red, dashed line) was produced using a one-dimensional model. A clumping factor of the He layer of $\zeta \sim 100$ was used. While the $H\alpha$ emission is produced by tiny fractions of H in the He layer below 12000 km s^{-1} , the double-peaked profile of the [O I] $\lambda\lambda$ 6300, 6363 doublet is again produced by $H\alpha$ absorption between 12000 and 12500 km s^{-1} (also see Figure 3).

Their analytical estimates do not depend on the SN 1993J model explicitly and should be valid for any SN IIb with moderate amounts of H ($\sim 0.1 M_{\odot}$). One may therefore conclude that the same mechanism operating in SN 1993J is also at work in SNe 2007Y and 2008ax. However, for SN 2008ax there are several problems connected to the shock-interaction interpretation of its $H\alpha$ nebular emission [Tau10]. In SN 2007Y shock interaction is not expected at all (Chevalier & Soderberg 2010).

In this section we present an alternative mechanism for powering late nebular $H\alpha$ emission. This mechanism may ex-

plain how late-time $H\alpha$ emission can be powered by radioactive decay without any need for shock interaction, solving the problems mentioned above. This mechanism is simple but needs special conditions to operate, which could explain why strong nebular $H\alpha$ emission is rare in stripped CC-SNe (this may also be explained by shock interaction).

We assume that a small fraction of hydrogen (of the order of 1%) is mixed into a helium-dominated layer. The degree of H ionisation will lie between 1 and almost 100% depending on the ionisation state of helium, since He recombination can ionise hydrogen strongly (see Appendix A). There is a sharp transition between complete and almost no ionisation of hydrogen, if the hydrogen mass is comparable to the mass of He II. In such a situation, when the degree of ionisation of helium decreases with time, as it does naturally, large amounts of neutral hydrogen can be produced in regions where no H I had been present at earlier epochs (this is explained in more detail in Appendix A). Therefore, the H I fraction in the He dominated layer can increase from approximately zero to, say, 2% of the total mass within several hundred days. Up to this epoch an observer would not even know about hydrogen in these regions since H II cannot be observed, except by extremely weak recombination radiation.

It is important to note that the energy deposited in the He-rich regions (at least in SN 2008ax, but probably also in SNe 1993J and 2007Y) is ~ 10 times larger than the energy emitted in $H\alpha$. This means that if only 10% of the deposited energy was transformed into $H\alpha$, shock interaction would not be needed to explain the late-time $H\alpha$ emission.

Under typical nebular conditions $\sim 70\%$ of the energy deposited in a He rich layer by radioactive decay is stored in thermal electrons. It is therefore clear that emission from this region is dominated by thermal electron collisional excitation and not by recombination. If heavy elements (C, O, Na, etc.) are mixed into the He layer in sufficient fractions, they can be excited by thermal electrons and cool the gas efficiently. In this case $H\alpha$ is predominantly produced by recombination, which is much too weak to explain the late time $H\alpha$ flux [Hou96; they neglected thermal electron excitation of hydrogen]. Since this scenario would produce high-velocity optical lines (e.g. oxygen or sodium), which are not observed, helium cannot be mixed with heavy elements strongly (at least in SN 2008ax; see Section 3).

If the gas consists of hydrogen and helium only, or if heavier elements are singly ionised to almost 100%, which would be the case if the fraction of these elements was lower than the fraction of He II, thermal electrons cannot cool effectively until they reach high enough temperatures to excite hydrogen ($\sim 10000\text{K}$; see Appendix A). In this scenario 99% of the thermal electron energy is radiated away by Ly α emission and therefore lost to the UV. About 1% is converted into $H\alpha$, which is too small by a factor of ~ 10 to explain the $H\alpha$ observations.

At this point clumping could become important. We use the symbol ζ for the clumping factor, which is defined as the inverse of the filling factor [see Maurer & Mazzali (2010) for more details]. A clumping factor ζ means that the density is increased by a factor of ζ locally, while the global density remains constant.

A helium layer containing small amounts of hydrogen can emit much more than 1% of its thermal electron energy

in H α if clumping is strong, since clumping increases the excitation of H I to $n = 2$ & 3, and the self-absorption optical depth of the H I ground state transitions.

Summarising, this means that, if hydrogen and helium are mixed in suitable fractions and clumped strongly, radioactive energy deposition can power H α completely without any additional source of energy. We present some estimates here, which support this idea.

Since the excitation potential of hydrogen is ~ 10 eV lower than that of helium, the thermal electron collisional excitation rates of hydrogen are approximately $\exp(10\text{eV}/kT) \sim 10^{5-3}$ times (at 10000 – 20000K) higher than those of helium. Unless there are $\sim 10^{5-3}$ times more He I than H I atoms $\sim 70\%$ of the total energy deposited in helium will be radiated away by hydrogen and He IR lines (the other 30% will go into non-thermal electron excitation and recombination radiation, mainly UV).

It is clear that, as long as H is ionised completely ($\gg 99\%$), H α emission and scattering are extremely weak. There is no H α scattering since there is no Ly α self-absorption if there is no H I, which means that the H I $n = 2$ level is depopulated strongly. Moreover, there is almost no H α emission, since only $\sim 20\%$ of the deposited energy go into ionisation. This energy is mainly emitted by He I recombination radiation and Ly α , which means that the fraction of deposited energy emitted by H α is less than one percent. Thermal electrons cool predominantly by exciting He I, since the temperature increases to more than 15000K.

We derive a rough estimate for the dependence of H α emission on clumping. We consider effective recombination into the hydrogen levels $n = 2$ and 3, thermal electron (de-) excitation between the ground state and the levels $n = 2$ and $n = 3$, and radiative transitions from H I $n = 3$ to $n = 2$ and from $n = 2$ to $n = 1$. We neglect radiative transitions from H I $n = 3$ to $n = 1$, since this rate is small owing to self-absorption. We also neglect thermal excitation from H I to $n = 2$ to $n = 3$, which may contribute to the population of the H I $n = 3$ level but is less important than direct excitation from the ground state. We only consider the situation where enough H I is present to cool the gas efficiently ($\frac{n_{\text{H I}}}{n_{\text{He}}} > 0.1\%$), which means that the H I ground state transitions are highly self-absorbed.

To calculate the formation of H α the population of the $n = 2$ state of H I has to be estimated

$$\begin{aligned} n_{\text{H I},2} &\sim \frac{C_{12}\zeta[+If_2]}{A_{21}\tau_{21}^{-1}\zeta^{-1} + C_{21}\zeta} n_{\text{H I},1}, & \tau_{21} &\gg 1 \\ &\propto \zeta^2, & \zeta &\sim 1, C_{12} > I \\ &\propto \zeta^0, & \zeta &\gg 1 \end{aligned} \quad (1)$$

where C_{ij} are the thermal electron collisional rates between the $n = i$ and j states of H I (e.g. Callaway 1994), I is the total ionisation rate (non-thermal electrons and photo-ionisation; see Appendix A), f_n are the fractions of recombining electrons, cascading into the H I n states and

$$\tau_{21} = \frac{\lambda_{\text{Ly}\alpha}^3 t g_2 A_{21}}{8\pi g_1} n_{\text{H I},1}, \quad n_{\text{H I},1} \gg n_{\text{H I},2} \quad (2)$$

is the Sobolev optical depth of the H I ground state, with $\lambda_{\text{Ly}\alpha} \sim 1216$ Å the wavelength of Ly α , g_n the statistical weights of the n states of H I and A_{21} the radiative rate of Ly α . Depending on the number density of the H I ground

state the $n = 2$ state can be thermally populated ($C_{21}\zeta \gg \frac{A_{21}}{\tau_{21}\zeta}$) at moderate clumping factors ($\zeta \sim 10$) already. The H α optical depth is given by

$$\begin{aligned} \tau_{\text{H}\alpha} &\sim \frac{\lambda_{\text{H}\alpha}^3 t g_3 A_{32}}{8\pi g_2} n_{\text{H I},2}, & n_{\text{H I},2} &\gg n_{\text{H I},3} \\ &\propto \zeta^2, & \zeta &\sim 1 \\ &\propto \zeta^0, & \zeta &\gg 1 \end{aligned} \quad (3)$$

where $\lambda_{\text{H}\alpha} \sim 6563$ Å is the wavelength of H α and A_{32} is the radiative rate of H α . $\tau_{\text{H}\alpha}$ increases with clumping at low clumping factors, but then saturates as soon as the depopulation of the H I $n = 2$ level is dominated by collisional de-excitation. In rough approximation the ratio of the H α to the Ly α luminosity is given by

$$\begin{aligned} \frac{\text{H}\alpha}{\text{Ly}\alpha} &\sim \frac{E_{\text{H}\alpha}}{E_{\text{Ly}\alpha}} \frac{n_{\text{H I},3}}{n_{\text{H I},2}} \frac{A'_{32}}{A'_{21}} \\ &\sim \frac{E_{\text{H}\alpha}}{E_{\text{Ly}\alpha}} \frac{C_{13}\zeta[+If_3]}{C_{12}\zeta[+If_2]} \\ &\times \left(1 + \frac{C_{21}\tau_{21}\zeta^2}{A_{21}}\right) \left(1 + \frac{C_{31}\tau_{\text{H}\alpha}\zeta^2}{A_{32}[1 - \exp(-\tau_{\text{H}\alpha}\zeta)]}\right)^{-1} \quad (4) \\ &\sim 0.03 \cdot \exp\left(-\frac{E_{\text{H}\alpha}}{kT}\right), & \zeta &\sim 1, C_{1j} > I \\ &\sim F(T, n_e, n_{\text{H}}, n_{\text{H I}}, \zeta), & \zeta &\gg 1 \end{aligned}$$

where A'_{ij} denotes the self-absorbed radiative transition rates between the $n = i$ and j states of H I.

Clumping can increase the relative strength of H α significantly. High clumping factors ($\zeta \gg 1$) increase the H α optical depth less effectively than they do the H α luminosity, while moderate clumping factors increase both. An estimate for the time-dependent density $n_{\text{H I}}$ is available (see Appendix A).

A numerical computation of the processes described above can be performed using our nebular code. In Figures 7, 8 and 9 we show models of SN 1993J (363 days), 2007Y (288 days) and SN 2008ax (359 days) using the mechanism described above (radioactive decay energy; mixing of H and He; strong clumping). Since the late H α emission of SNe 2001ig and 2003bg is much weaker it is clear that the late H α emission of these SNe can be reproduced in a similar way. For SN 1993J we use the He mass estimate of Woosley et al. (1994). For SN 2007Y we assume that the He mass is a bit smaller than in SN 1993J. For SN 2008ax the He mass is estimated in Section 3. For SN 1993J we use a helium mass of $2 M_{\odot}$, a hydrogen mass of $0.2 M_{\odot}$ and a clumping factor $\zeta \sim 200$, for SN 2007Y we use a helium mass of $1.5 M_{\odot}$, a hydrogen mass of $0.1 M_{\odot}$ and a clumping factor $\zeta \sim 100$ and for SN 2008ax we use a helium mass of $2 M_{\odot}$, a hydrogen mass of $0.2 M_{\odot}$ and a clumping factor of $\zeta \sim 100$. Most of the hydrogen is concentrated in a thin shell at high velocities, while tiny fractions are mixed into the lower velocity helium. It is difficult to decide whether clumping, the helium or the hydrogen mass should be increased to obtain a reproduction of the spectra. Several combinations are possible. Additionally, the outer region could be influenced by shock interaction. Therefore it is not possible to derive a hydrogen or helium mass estimate from this procedure. It seems however clear that small amounts of hydrogen are sufficient to reproduce late H α emission (which is usually not possible [Hou96]), if there is strong clumping ($\zeta \sim 100$).

It is important to note that we could not reproduce the temporal evolution of the $H\alpha$ line using this mechanism with our nebular code. We can find models that reproduce the observations at any epoch, but no model describing the observations at all epochs consistently. This is discussed in Section 6.

6 DISCUSSION

6.1 Late $H\alpha$ emission

We have investigated the formation of $H\alpha$ in the nebular phase of five SNe I Ib (re-classifying SN 2007Y as SN I Ib). We find that radioactive energy from ^{56}Ni decay is not sufficient to power the $H\alpha$ emission observed at late nebular epochs (> 200 days), as long as the energy deposited in the He layer cannot be tapped. This finding is consistent with the work of [Hou96] for SN 1993J, but raises the question of which mechanism causes the observed $H\alpha$ flux.

In Section 5 we have shown that a combination of mixing and strong clumping could solve this problem. It is not clear whether such high clumping factors are realistic (however see e.g. Kozma & Fransson (1998)). Furthermore, we could not reproduce the temporal evolution of $H\alpha$ using this mechanism. This may be because of several reasons. First, there is a degeneracy between the hydrogen and the helium mass and clumping and it is not clear which combination has to be chosen. Secondly, as can be seen from Equation 4, the strength of $H\alpha$ is very sensitive to the electron density and temperature at clumping values of the order 100. In addition, $n_{\text{H}[I,II]}$ is extremely sensitive to mixing and clumping. The composition has to be known at the one percent level or better. Our nebular code is expected to be less accurate. We do not treat UV-radiation transport explicitly, the ionisation of hydrogen by helium is treated in approximation only and in general there are uncertainties owing to the atomic data and owing to the incomplete description of the physical scenario. Asymmetries of the ejecta can further complicate the problem.

Since the radioactive scenario appears to have problems, it may be worth considering the most common interpretation, i.e. that late SN I Ib $H\alpha$ emission is the result of shock interaction. An extensive discussion of several shock interaction scenarios for SN 2008ax can be found in [Tau10]. However, as pointed out by [Tau10], there are several problems within all these scenarios. Shock interaction has difficulties explaining why $H\alpha$ emission is observed at low velocities in SN 2007Y and SN 2008ax (see [Tau10]). Moreover, there are contradictions between X-ray and $H\alpha$ observations, if both are interpreted as shock interaction (see SNe 2003bg, 2007Y). These problems may arise from an incomplete understanding of the influence of the shock radiation on the ejecta or from an inaccurate treatment of the physical parameters determining the shock properties (e.g. the SN outer density structure).

The shock interaction model can explain why strong $H\alpha$ emission at late times is rare in SN I Ib and has the advantage that it may explain a flattening of the late $H\alpha$ light curve, which is observed in SN 1993J and possibly in SN 2008ax. However, this has never been shown quantitatively. Nor has it been shown that shock interaction can reproduce late $H\alpha$ emission in detail in any SN I Ib at all.

The mechanism presented in Section 5 can explain the formation of low velocity $H\alpha$ in SNe 2007Y and 2008ax, which is observed. It can further explain the absence of high velocity $H\alpha$ emission, again consistent with the observations, since in this scenario the $H\alpha$ emission traces the He distribution. It can explain why SN 2007Y, has strong $H\alpha$ emission, although Chevalier & Soderberg (2010) claim that there is extremely weak shock interaction in SN 2007Y. It can explain why SN 2003bg has no strong $H\alpha$ emission, although Chevalier & Soderberg (2010) claim that there is strong shock interaction in SN 2003bg. Since the model needs some fine tuning it can explain why strong late time $H\alpha$ is rare in SNe I Ib.

There may well be some other mechanism (not clumping; still mixing of H and He), which emits in $H\alpha$ energy absorbed by the He layer. If it was possible to use $\sim 10\%$ of the energy of a massive He shell to excite $H\alpha$ without producing any other strong optical lines, the late-time $H\alpha$ emission could be explained by radioactive energy deposition alone.

6.2 Nebular line profiles of SNe I Ib

Usually, double-peaked line profiles are interpreted as toroidal ejecta distributions. While we agree with this interpretation in general (e.g. for SN Ib/c; see also Section 3) we think that the situation may be different in SNe I Ib. We have shown that, taking the 40 day (after explosion) $H\alpha$ absorption minimum velocity as lower boundary of the bulk of hydrogen (as it is usually done) we can explain the peak profile of the [O I] $\lambda\lambda$ 6300, 6363 doublet for all five SNe of our sample consistently by $H\alpha$ absorption.

Since $H\alpha$ absorption causes a split of the [O I] $\lambda\lambda$ 6300, 6363 doublet if it is located around 12000 km s^{-1} , and since the position of $H\alpha$ influences the position of this split, we can infer the radial distribution of H I from fitting the [O I] $\lambda\lambda$ 6300, 6363 doublet profile. For all five SNe of our sample the $H\alpha$ velocity measured with this method agrees very well with the early-time $H\alpha$ minimum velocity (see Table 3). It seems unlikely that this is coincidence.

The outer $H\alpha$ region could be optically thick even at late epochs (e.g. excited by shock interaction), which could explain why the profile of the [O I] $\lambda\lambda$ 6300, 6363 doublet does not change its shape significantly at late epochs. For example, the reverse shock of SN 2008ax could be located around 12000 km s^{-1} at 359 days after the explosion [Tau10].

6.3 SN 2008ax

We have derived a three-dimensional model of SN 2008ax. Two kinds of asymmetries may be observed. First the He IR lines are double-peaked, which is most easily explained by a torus shaped He distribution. Secondly, the blue sides of the He lines appear to be stronger than the red sides.

We find a total ejecta mass of $\sim 3 M_{\odot}$, containing about $0.1 M_{\odot}$ of ^{56}Ni and expanding with a kinetic energy of $\sim 10^{51}$ ergs, which is consistent with findings from light curve and early-time $H\alpha$ absorption modelling (Table 2; also see [Tau10]). We find a helium mass of $\sim 2 M_{\odot}$ and derive the abundances of heavier elements such as carbon or oxygen (Table 1).

While most of the heavy element mass is confined to velocities below 4500 km s^{-1} , helium is predominantly found between 4500 and probably 12000 km s^{-1} . The outer boundary is uncertain. Some helium is present below 4500 km s^{-1} . We find that a separation of helium and heavy elements, at least between 2000 and 4500 km s^{-1} , improves the reproduction of the He IR lines.

Since our nebular code does not reproduce the continuum flux observed around 20000 \AA , we added some artificial background to allow He I 20587 \AA line scattering. There seems to be no He I 20587 \AA line scattering above $\sim 10000 \text{ km s}^{-1}$, while the He I 10830 \AA line would not be in conflict with higher helium velocities. The observations of the He I 20587 \AA line place an upper limit on the He mass between 9500 and 12000 km s^{-1} of $\sim 0.05 M_{\odot}$. It may well be that continuum destruction (e.g. by hydrogen), which could reduce the He I 20587 \AA optical depth, is important. In this case the He mass in this region could be larger.

We can compare our results to SN IIB models of Nomoto et al. (1993) and Woosley et al. (1994). The Nomoto et al. (1993) models [also see Hou96] predict a strong confinement of ^{56}Ni to low velocities ($< 2000 \text{ km s}^{-1}$). Other heavy elements are distributed in layers above the radioactive core. Most of the hydrogen is confined to a thin layer above the He layer. This He layer contains some traces of hydrogen and heavier elements. The models of Woosley et al. (1994) predict a broader distribution of ^{56}Ni in velocity space. Heavy elements dominate at low velocities but are also mixed into the He layer. Helium and hydrogen are mixed in the outer regions.

We find that ^{56}Ni is probably not as centrally confined as predicted by the Nomoto et al. (1993) models. On the other hand carbon seems to be confined to a thin shell on top of the iron core in agreement with these models. Since our core is deformed to an axis ratio of $\sim 3:2$ (see Figure 1), one probably cannot expect perfect agreement with the spherical symmetric models. The distribution of heavy elements seems rather consistent with the predictions in the core as well as in the He layers. Our results for hydrogen are inaccurate and therefore a comparison is difficult.

We compare the masses of He, C, O, Ca and ^{56}Ni of our SN 2008ax model to the 13C model of Woosley et al. (1994), which has been used by Tsvetkov et al. (2009) to reproduce the light curve of SN 2008ax. We find that our estimates of the He, C, Ca and ^{56}Ni mass agree at the 10% level. The estimate of the oxygen mass is larger by a factor of ~ 2 than predicted by the 13C model.

Thanks to its late time IR observations, SN 2008ax is the first SN IIB where the He density field can be determined from nebular observations. Other methods, such as light-curve modelling, provide poor information about element abundances or asphericities. Early-time modelling can determine the properties of the outer layers more accurately, but no information about the central region can be obtained. Therefore nebular IR observations (10000 to 22000 \AA) of SNe Ib and IIB are highly desirable.

7 SUMMARY & CONCLUSION

We have derived estimates related to hydrogen and helium line formation in the nebular phase of SNe IIB. We have

shown that hydrogen can be highly ionised if it is mixed with helium in suitable ratios. This has probably been known before. However, it could explain why H α can sometimes be observed in the nebular phase but not at early times. This finding is of special interest for SN 2007Y.

From our analysis it seems likely that SN 2007Y is a SN IIB. The lack of strong H α absorption around 50 days after explosion may well be explained by strong mixing of H and He. Such mixing could also explain the formation of strong late time H α . Since we cannot determine the He distribution of SN 2007Y, this remains a speculation.

We have shown that radioactive energy deposition is insufficient to produce the late-time H α emission in all SNe IIB of our sample, as long as the energy of the helium layer cannot be tapped by H α .

Shock interaction may be observed in all SNe of our sample. There seem to be two types of late H α emission scenarios. Strong, box-shaped (SNe 1993J, 2007Y, 2008ax) and weak (SNe 2001ig, 2003bg) H α . The simplest explanation would seem to be strong and weak shock interaction, respectively. However, this is in conflict with findings of Chevalier & Soderberg (2010), at least for SNe 2003bg and 2007Y. It also seems difficult to explain the low velocity observations in H α by shock interaction [Tau10].

We presented an alternative mechanism to shock interaction, explaining late time H α emission by radioactive energy deposition. The right combination of mixing and clumping of hydrogen and helium has been shown to be able to reproduce the H α observations of all SNe of our sample at least up to 350 days after explosion. However, there are also some problems with this interpretation of late H α emission. Summarising, it is not clear how late H α is formed in SNe IIB. Therefore, we were not able to derive an estimate of the hydrogen mass for any SN of our sample.

We have shown that most likely the profile of the [O I] $\lambda\lambda 6300, 6363$ doublet is influenced by H α absorption strongly. Hydrogen concentrations above $\sim 11000 \text{ km s}^{-1}$ can cause double-peaked oxygen profiles, while slower hydrogen can not. We have shown that observations of early-time H α absorption minima and the corresponding oxygen line profiles are perfectly consistent with this interpretation for all five SNe of our sample.

This scenario also explains why other lines, like Ca II or [O I] 5577 \AA , are single peaked in all SNe of our sample. An exception are the He lines of SN 2008ax, which show signs of asymmetry. It seems likely that at least the inner part of SN 2008ax is asymmetric. We have obtained a three-dimensional model of the SN 2008ax envelope. For the first time the helium mass of a SN IIB has been determined from nebular modelling. We have obtained estimates of the total mass and kinetic energy of SN 2008ax in excellent agreement with results from light-curve modelling. Chemical abundances have been derived. The nebular model of SN 2008ax provides the opportunity to compare observations and theoretical SN IIB models with unprecedented richness of detail.

As already stated by Houck & Fransson (1996), nebular IR observations (10000 to 22000 \AA) of core-collapse SNe would be extremely useful for deriving properties of CC-SNe such as helium abundance, total mass and kinetic energy. It is important that both He IR lines (10830 and 20587 \AA) are observed simultaneously. Such observations should be obtained for any SN Ib or IIB.

REFERENCES

- Aldering G., Humphreys R. M., Richmond M., 1994, *AJ*, 107, 662
- Axelrod T. S., 1980, Ph.D. thesis, California Univ., Santa Cruz.
- Bates D. R., Damgaard A., 1949, *Philosophical Transactions of the Royal Society of London. Series A, Mathematical and Physical Sciences*, 242, 842, 101
- Berrington K. A., Kingston A. E., 1987, *J. Phys. B: At. Mol. Phys.*, 20, 6631
- Burgess A., 1965, *MmRAS*, 69, 1
- Burgess A., Seaton M. J., 1960, *MNRAS*, 120, 121
- Callaway J., 1994, *Atomic Data and Nuclear Data Tables*, 57, 9
- Chevalier R. A., 1981, *ApJ*, 251, 259
- Chevalier R. A., Soderberg A. M., 2010, *ApJ*, 711, L40
- Chornock R., Filippenko A. V., Li W., et al., 2010, *ArXiv e-prints*
- Chugai N. N., 1987, *Astrophysics*, 26, 53
- Chugai N. N., 1991, *MNRAS*, 250, 513
- Crockett R. M., Eldridge J. J., Smartt S. J., et al., 2008, *MNRAS*, 391, L5
- Drake G. W., Victor G. A., Dalgarno A., 1969, *Physical Review*, 180, 25
- Eldridge J. J., Vink J. S., 2006, *A&A*, 452, 295
- Filippenko A. V., 1997, *ARA&A*, 35, 309
- Filippenko A. V., Matheson T., Barth A. J., 1994, *AJ*, 108, 2220
- Fransson C., 1994, in *Circumstellar Media in Late Stages of Stellar Evolution*, edited by R. E. S. Clegg, I. R. Stevens, & W. P. S. Meikle, 120–+
- Fransson C., Björnsson C., 1998, *ApJ*, 509, 861
- Fransson C., Björnsson C., 2005, in *IAU Colloq. 192: Cosmic Explosions, On the 10th Anniversary of SN1993J*, edited by J.-M. Marcaide & K. W. Weiler, 59–+
- Grassberg E. K., Imshennik V. S., Nadyozhin D. K., 1971, *Ap&SS*, 10, 28
- Hamuy M., Deng J., Mazzali P. A., et al., 2009, *ApJ*, 703, 1612
- Höflich P., 1991, *A&A*, 246, 481
- Houck J. C., Fransson C., 1996, *ApJ*, 456, 811
- Kotak R., Vink J. S., 2006, *A&A*, 460, L5
- Kozma C., Fransson C., 1998, *ApJ*, 497, 431
- Li H., McCray R., 1995, *ApJ*, 441, 821
- Lucy L. B., 1991, *ApJ*, 383, 308
- Maeda K., Kawabata K., Mazzali P. A., et al., 2008, *Science*, 319, 1220
- Matheson T., Filippenko A. V., Barth A. J., et al., 2000, *AJ*, 120, 1487
- Maund J. R., Smartt S. J., 2009, *Science*, 324, 486
- Maund J. R., Smartt S. J., Kudritzki R. P., Podsiadlowski P., Gilmore G. F., 2004, *Nature*, 427, 129
- Maund J. R., Wheeler J. C., Patat F., Wang L., Baade D., Höflich P. A., 2007, *ApJ*, 671, 1944
- Maurer J. I., Mazzali P. A., 2010, submitted to *MNRAS*
- Maurer J. I., Mazzali P. A., Deng J., et al., 2010, *MNRAS*, 402, 161
- Mazzali P. A., Deng J., Hamuy M., Nomoto K., 2009, *ApJ*, 703, 1624
- Mazzali P. A., Kawabata K. S., Maeda K., et al., 2005, *Science*, 308, 1284
- Mazzali P. A., Kawabata K. S., Maeda K., et al., 2007, *ApJ*, 670, 592
- Mazzali P. A., Nomoto K., Patat F., Maeda K., 2001, *ApJ*, 559, 1047
- Milisavljevic D., Fesen R. A., Gerardy C. L., Kirshner R. P., Challis P., 2010, *ApJ*, 709, 1343
- Modjaz M., Kirshner R. P., Blondin S., Challis P., Matheson T., 2008, *ApJ*, 687, L9
- Nomoto K., Suzuki T., Shigeyama T., Kumagai S., Yamaoka H., Saio H., 1993, *Nature*, 364, 507
- Nymark T. K., Chandra P., Fransson C., 2009, *A&A*, 494, 179
- Pastorello A., Kasliwal M. M., Crockett R. M., et al., 2008, *MNRAS*, 389, 955
- Patat F., Chugai N., Mazzali P. A., 1995, *A&A*, 299, 715
- Roming P. W. A., Pritchard T. A., Brown P. J., et al., 2009, *ApJ*, 704, L118
- Rozsnyai B. F., Jacobs V. L., Davis J., 1980, *Phys. Rev. A*, 21, 6, 1798
- Ruiz-Lapuente P., Lucy L. B., 1992, *ApJ*, 400, 127
- Ryder S. D., Murrowood C. E., Stathakis R. A., 2006, *MNRAS*, 369, L32
- Scholz T. T., Walters H. R. J., Burke P. J., Scott M. P., 1990, *MNRAS*, 242, 692
- Seaton M. J., 1958, *MNRAS*, 118, 504
- Silverman J. M., Mazzali P., Chornock R., et al., 2009, *PASP*, 121, 689
- Soderberg A. M., Chevalier R. A., Kulkarni S. R., Frail D. A., 2006, *ApJ*, 651, 1005
- Stritzinger M., Mazzali P., Phillips M. M., et al., 2009, *ApJ*, 696, 713
- Suzuki T., Nomoto K., 1995, *ApJ*, 455, 658
- Taubenberger S., Navasardyan H., Maurer J. I., et al., 2010, submitted to *MNRAS*
- Taubenberger S., Valenti S., Benetti S., et al., 2009, *MNRAS*, 397, 677
- Tsvetkov D. Y., Volkov I. M., Baklanov P., Blinnikov S., Tuchin O., 2009, *Peremennye Zvezdy*, 29, 2
- Utrobin V., 1994, *A&A*, 281, L89
- van Dyk S. D., Weiler K. W., Sramek R. A., Rupen M. P., Panagia N., 1994, *ApJ*, 432, L115
- van Regemorter H., 1962, *ApJ*, 136, 906
- Woosley S. E., Eastman R. G., Weaver T. A., Pinto P. A., 1994, *ApJ*, 429, 300
- Xu Y., McCray R., 1991, *ApJ*, 375, 190

APPENDIX A

Hydrogen ionisation in a He-dominated layer

We derive some estimates for the ionisation of hydrogen by non-thermal electrons and by the UV-radiation emitted by helium. We assume that H is mixed with He but not with other elements. Therefore the treatment presented is only valid if heavy elements are present in smaller fractions than hydrogen and helium. However, other elements with ionisation potentials below ~ 20 eV would be affected in a way similar to hydrogen.

About 40% of all helium recombinations go directly to the ground state and cause another ionisation of helium and possibly of hydrogen. This recycling process increases the

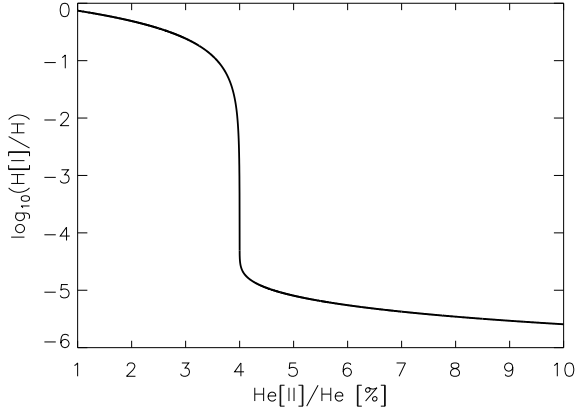


Figure 10. The logarithmic fraction of neutral hydrogen $\frac{n_{\text{H}[I]}}{n_{\text{H}}}$ (full black line; Equation 10) as a function of the He II fraction $\frac{n_{\text{He}[II]}}{n_{\text{He}}}$ [%] for a helium dominated layer containing 2% of hydrogen, assuming $f = 0.5$ and $\xi_{\text{H}} = 0.1$. The He density was set to 10^8 g cm^{-3} . There is a steep decrease of H I as soon as the fraction of He II increases above $\frac{2}{7}$ %. Changing the degree of ionisation of He by 1% only (from 4.5 to 3.5% in this example), the fraction of H I increases by a factor of 10^4 .

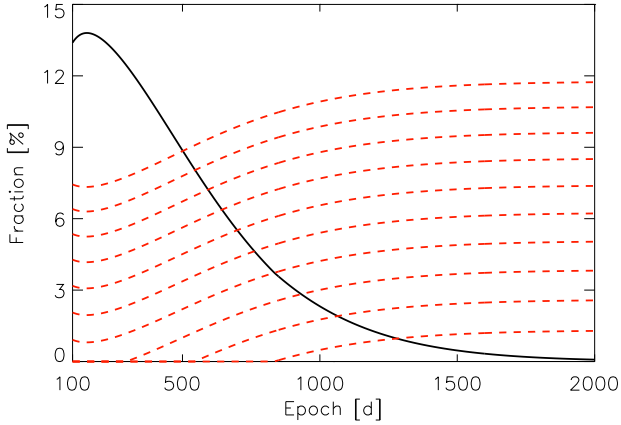


Figure 11. Toy model of a SN I Ib. The time-dependent fraction $\frac{n_{\text{He}[II]}}{n_{\text{He}}}$ [%] (full black line; Equation 15) is shown for a model described in the text ($M_{\text{He}} = 3 M_{\odot}$, $M_{\text{Ni}} = 0.1 M_{\odot}$, $f = 0.5$, $T = 15000\text{K}$). The fraction $\frac{n_{\text{H}[I]}}{n_{\text{H}}}$ [%] (dashed red line; Equation 10) is shown for hydrogen masses of 0.01 to $0.1 M_{\odot}$ (bottom to top). There is no clumping of the H and He layer. The calculation starts at 100 days since at earlier epochs photospheric radiation may be important for ionising hydrogen and helium and our estimates become invalid. Although the model is highly simplified it demonstrates that depending on the ratio of hydrogen and helium the H I fraction can be approximately zero for the first 100 days and can increase rapidly at later epochs. This means that no H α would be observed at early epochs, while strong H α emission or scattering is possible later.

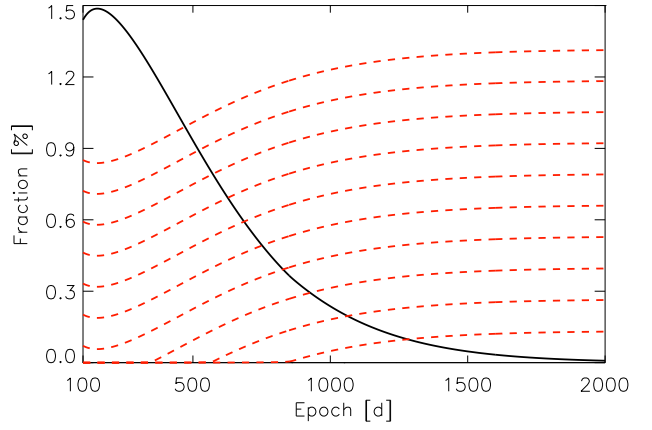


Figure 12. Toy model of a SN I Ib. The time-dependent fraction $\frac{n_{\text{He}[II]}}{n_{\text{He}}}$ [%] (full black line; Equation 15) is shown for a model described in the text ($M_{\text{He}} = 3 M_{\odot}$, $M_{\text{Ni}} = 0.1 M_{\odot}$, $f = 0.5$, $T = 15000\text{K}$). The fraction $\frac{n_{\text{H}[I]}}{n_{\text{H}}}$ [%] (dashed red line; Equation 10) is shown for hydrogen masses of 0.001 to $0.01 M_{\odot}$ (bottom to top). The clumping factor of the H and He layer is set to 100, which reduces the degree of ionisation strongly. The calculation starts at 100 days since at earlier epochs photospheric radiation may be important for ionising hydrogen and helium and our estimates become invalid. Although the model is highly simplified it demonstrates that depending on the ratio of hydrogen and helium the H I fraction can be approximately zero for the first 100 days and can increase rapidly at later epochs. This means that no H α would be observed at early epochs, while strong H α emission or scattering is possible later.

total ionisation rate but is not important for the rest of the appendix.

Electrons recombining to an excited state reach the ground state by two-photon emission (2PE) of the $2s(^1S)$ state during the nebular phase. At early times, when the 2p levels are strongly excited by radiation, most electrons reach the ground state via the 2p levels.

In the case of 2PE approximately 30% of the ground state transition radiation can ionise hydrogen (the two photons are created with energies between 0 and 20.6 eV; the chance of producing a photon with $E > 13.6 \text{ eV}$ is $\sim 30\%$; Drake et al. 1969) and in the case of 2p transitions 100%. Therefore, we assume that a fraction f (0.3 – 1.0) of all He recombinations into excited states can ionise a hydrogen atom.

The total ionisation rate of hydrogen is then determined by non-thermal electron ionisation and by radiative ionisation from He recombination radiation. The non-thermal electron ionisation rates of neutral hydrogen and helium are given by (e.g. Axelrod 1980)

$$Y = Y_{\text{H}[I], \text{He}[I]} = \frac{L_{\text{Dep}}}{N_{\text{Tot}} W_{\text{H}[I], \text{He}[I]}} \quad (5)$$

where N_{Tot} is the total number of atoms and $W_{\text{H}[I], \text{He}[I]}$ is the work per ion of hydrogen and helium, which depends on the ratio of electrons to atoms and on the absolute atomic density (weakly).

For simplicity we assume $W_{\text{H}[I]} = W_{\text{He}[I]}$ in this section,

which will cause an error of $\sim 30\%$ on the ionisation rates of H and He in the worst case.

During the first few hundred days the SN is in ionisation equilibrium (e.g. Axelrod 1980) and the ionisation balance of hydrogen can be estimated as

$$Y(n_{\text{He}[I]}D_{\text{H}[I]}f + n_{\text{H}[I]}) = R_{\text{H}[I]}(n_{\text{He}[II]} + n_{\text{H}[II]})\zeta n_{\text{H}[II]} \quad (6)$$

where $D_{\text{H}[I]}f$ is the fraction of He recombination radiation ionising hydrogen with

$$D_{\text{H}[I]} = 1 - \exp(-\sigma_{\text{H}}\Delta R n_{\text{H}[I]}) \quad (7)$$

where σ_{H} is the ionisation cross-section of H at ~ 20 eV and ΔR is some characteristic width of the He shell. The ionisation balance of Helium can be written as

$$Y n_{\text{He}[I]} = R_{\text{He}[I]}(n_{\text{He}[II]} + n_{\text{H}[II]})\zeta n_{\text{He}[II]} \quad (8)$$

Setting $R = R_{\text{H}[I]} = R_{\text{He}[I]}$ (which is a good approximation) one obtains

$$D_{\text{H}[I]}n_{\text{He}[I]}f + n_{\text{H}[I]} = \frac{n_{\text{He}[I]}}{n_{\text{He}[II]}}(n_{\text{H}} - n_{\text{H}[I]}) \quad (9)$$

The exact solution of Equation 9 is given by

$$n_{\text{H}[I]} = \xi_{\text{H}}^{-1} W \left(\frac{n_{\text{He}[I]}n_{\text{He}[II]}}{n_{\text{He}}} \xi_{\text{H}} f \exp \left[- \frac{n_{\text{He}[I]} \xi_{\text{H}} (n_{\text{H}} - f n_{\text{He}[II]})}{n_{\text{He}}} \right] \right) + \frac{n_{\text{He}[I]}}{n_{\text{He}}} (n_{\text{H}} - f n_{\text{He}[II]}) \quad (10)$$

where $W(x) \equiv \sum_{n=1}^{\infty} \frac{(-n)^{n-1}}{n!} x^n$ is the Lambert W function. In approximation, the deposition fraction $D_{\text{H}[I]}$ is given by

$$D_{\text{H}[I]} = \begin{cases} 1 & \sigma_{\text{H}}\Delta R n_{\text{H}[I]} \gg 1 \\ \sigma_{\text{H}}\Delta R n_{\text{H}[I]} \equiv \xi_{\text{H}} n_{\text{H}[I]} & \sigma_{\text{H}}\Delta R n_{\text{H}[I]} \ll 1 \end{cases}$$

The ionisation cross section of hydrogen is $\sim 2 \cdot 10^{-18}$ cm² at 20 eV and the SN radius is of the order of 10^{16} cm during the first few hundred days, which means that ξ_{H} will be of order $0.01 - 0.1$ cm³. The number density of neutral hydrogen is then given by

$$\frac{n_{\text{H}[I]}}{n_{\text{H}}} = \begin{cases} \frac{n_{\text{He}[I]}}{n_{\text{He}}} \left(1 - f \frac{n_{\text{He}[II]}}{n_{\text{H}}} \right) & \xi_{\text{H}} n_{\text{H}[I]} \gg 1 \\ \frac{n_{\text{He}[I]}}{n_{\text{He}} + n_{\text{He}[I]} n_{\text{He}[II]} f \xi_{\text{H}}} \sim (f n_{\text{He}[II]} \xi_{\text{H}})^{-1} & \xi_{\text{H}} n_{\text{H}[I]} \ll 1 \end{cases}$$

The degree of ionisation of hydrogen increases rapidly as soon as the hydrogen number density becomes similar to the number density of He II times f (see Figure 10).

A factor of 10 or less in the hydrogen abundance can make a difference of several orders in magnitude in the degree of ionisation. Also, a small change in the ionisation balance of He can have serious influence on the ionisation balance of H. A simple example is given by a helium layer containing 2% hydrogen and $\frac{2.5}{f}\%$ He II. Hydrogen is ionised to $\gg 99\%$ then. If the amount of He II decreases to $\frac{1.5}{f}\%$ (a decrease of the ionisation fraction is expected at late epochs; see Figures 11 and 12) the H II fraction decreases to less than 10%. **Without changing the physical conditions significantly, the fraction of H I can change by several orders in magnitude.**

Toy model of a SN IIB

To obtain some rough estimate of the electron temperature in a He-dominated layer containing some small fraction

of hydrogen, we calculate the temperature-dependent ratio of collisional excitation and recombination \mathcal{R} . The thermal electron excitation coefficient from $n = 2$ to $n = 1$ is given by

$$C_{12} \sim 8.6 \times 10^{-6} \frac{n_e}{T^{1/2}} \frac{\Omega_{21}}{g_1} \exp\left(-\frac{E_{\text{Ly}\alpha}}{kT}\right) \equiv C_0 n_e \quad (11)$$

where Ω_{21} is the effective collision strength of the hydrogen $n = 1$ to $n = 2$ transitions given by Scholz et al. (1990) and f_2, g_1 are defined in Section 5. This gives

$$\mathcal{R} = \frac{C_{12} \zeta n_{\text{H}[I]}}{R n_e \zeta n_{\text{H}[II]} f_2} = \frac{C_0}{R f_2} \left(\frac{n_{\text{H}}}{n_{\text{H}[I]}} - 1 \right)^{-1} \quad (12)$$

While C_0 increases with temperature R decreases and $\frac{C_0}{R f_2}$ is approximately one at ~ 11000 K. Since hydrogen must be excited by thermal collisions effectively in order to produce a significant contribution to the total luminosity, \mathcal{R} must be larger than $\gg 1$. Therefore the temperature must be higher than ~ 10000 K, depending on the H I fraction.

At temperatures of ~ 20000 K (which are reached for low fractions $\frac{n_{\text{H}[I]}}{n_{\text{H}}} < 0.1$; this implies $n_{\text{H}[I]} \leq n_{\text{He}[II]} \ll n_{\text{He}[I]}$) thermal excitation of He becomes important, the above estimate becomes invalid and the relative importance of H I emission decreases as compared to He I. Therefore, the temperature should be $\sim 10000 - 15000$ K in order to allow effective H I emission.

We can use this temperature estimate to calculate the temporal evolution of He II and therefore H I for a toy model of the SN ejecta. Of course this temperature estimate is not exact, but it is sufficient to demonstrate how the absolute fraction $\frac{n_{\text{H}[I]}}{n_{\text{H}} + n_{\text{He}}}$ in a helium dominated layer can evolve with time (see Figures 11 and 12).

The deposited energy can be estimated analytically if the He density is known. For simplicity we assume that X solar masses of He and Y solar masses of ^{56}Ni are distributed within a sphere of velocity v homogeneously (of course this is in conflict with our assumption that He is mixed with small fractions of heavy elements only, but this is a toy model only and He and ^{56}Ni could be separated on small scales). At nebular epochs (say, > 100 days), when most of ^{56}Ni has decayed to ^{56}Co , the deposited luminosity is given by

$$L_{\text{Dep}}(t) \sim 1.3 \times 10^{43} \exp\left(-\frac{t[\text{d}]}{111.4}\right) M_{^{56}\text{Ni}}[M_{\odot}] f_{\text{Dep}} \text{ ergs s}^{-1} \quad (13)$$

where f_{Dep} is the deposition function, which can be calculated analytically for a homogeneous sphere (e.g. Axelrod 1980). For three solar masses of helium and a ^{56}Ni mass of $\sim 0.1 M_{\odot}$ distributed homogeneously in a sphere of 10000 km s^{-1} the luminosity deposited around 350 days is $\sim 10^{39.5} \text{ ergs s}^{-1}$ while the $\text{H}\alpha$ luminosity of SN 2008ax at this epoch is $\sim 10^{38.5} \text{ ergs s}^{-1}$ only [Tau10].

Since the ionisation potential of He is high and since we assumed that it is the predominant element, helium is mainly ionised by non-thermal electrons

$$\mathcal{R}_{\text{He}} Y_{\text{He}} n_{\text{He}[I]} = R_{\text{He}} \zeta (n_{\text{He}[II]} + n_{\text{H}[II]}) n_{\text{He}[II]} \quad (14)$$

where $\mathcal{R}_{\text{He}} \sim 1.5$ is the recycling fraction of helium. This

gives

$$\frac{n_{\text{He[II]}}}{n_{\text{He}}} \sim \frac{R_{\text{He}}\zeta n_{\text{H[II]}} + \mathcal{R}_{\text{He}}Y_{\text{He}}}{2R_{\text{He}}\zeta n_{\text{He}}} \times \left(-1 + \sqrt{1 + 4 \frac{\mathcal{R}_{\text{He}}Y_{\text{He}}R_{\text{He}}\zeta n_{\text{He}}}{(R_{\text{He}}\zeta n_{\text{H[II]}} + \mathcal{R}_{\text{He}}Y_{\text{He}})^2}} \right) \quad (15)$$

We compute Equations 10 and 15 for the toy model described above. We assume that 50% of all He recombinations into excited states can ionise a hydrogen atom ($f = 0.5$) and vary the hydrogen mass between 0.01 and 0.1 M_{\odot} . The temporal evolution of the H I fraction is shown in Figure 11. Depending on the ratio of hydrogen and helium the fractions of H I can increase dramatically between 100 and 1000 days. This means that H α scattering or emission can appear at late epochs, without any hydrogen being detected at earlier times. In Equation 10 and 15 we assumed ionisation equilibrium, which may become invalid at epochs of ~ 500 days and later. Therefore, we underestimate the He [II] fraction at very late epochs. However, qualitatively the effect is the same, since H I ionisation is related to He II recombination even at 1000 days and later.